

Advantages of superconducting quantum interference device-detected magnetic resonance over conventional high-frequency electron paramagnetic resonance for characterization of nanomagnetic materials

Brant Cage^{a)} and Stephen E. Russek
National Institute of Standards and Technology, Boulder, Colorado 80305

David Zipse and Naresh S. Dalal
Florida State University, Tallahassee, Florida 32306

(Presented on 10 November 2004; published online 16 May 2005)

A dc-detected high-frequency electron paramagnetic resonance (HF-EPR) technique, based on a standard superconducting quantum interference device (SQUID) magnetometer, has significant advantages over traditional HF-EPR based on microwave absorption measurements. The SQUID-based technique provides *quantitative* determination of the dc magnetic moment as a function of microwave power, magnetic field and temperature. The EPR spectra obtained do not contain variability in the line shape and splittings that are commonly observed in the standard single-pass transmission mode HF-EPR. We demonstrate the improved performance by comparing EPR spectra for Fe8 molecular nanomagnets using both SQUID-based and conventional microwave-absorption EPR systems. © 2005 American Institute of Physics.

[DOI: 10.1063/1.1850816]

I. INTRODUCTION

High-frequency electron paramagnetic resonance (HF-EPR) has proved to be an invaluable technique for characterization of magnetic materials.¹⁻⁷ HF-EPR is generally performed using one of two configurations. In the first,^{3,4,6} the sample is contained within a resonant cavity and the change in quality factor (Q) is measured, from which the out-of-phase imaginary (absorption) component of the complex volume microwave susceptibility is determined, χ'' , or the change in resonant frequency of the cavity is measured, from which the in-phase real (dispersion) component χ' is derived. The second configuration is a single-pass or transmission measurement where the sample is mounted inside a waveguide and the change in transmitted radiation power is measured as a function of the swept magnetic field.^{2,5,7} The former has the advantage of high sensitivity and discrete observation of χ' and χ'' , whereas the latter has the advantage of broadband measurements and ease of use. Unfortunately, discrete line shape analysis of the transmission technique is hindered by admixtures of absorptive and dispersive signals as well as effects related to the microwave propagation.⁷

In general, for an exchange-coupled spin system, the EPR signal tends towards a Lorentzian line shape. Following Pake and Purcell⁸ in Fig. 1 we analyze the complex magnetic susceptibility, χ , where $\chi = \chi' + i\chi''$ in terms of the dimensionless parameter x such that $x = 2(H_0 - H) / \Delta H_{1/2}$ where H_0 , H and $\Delta H_{1/2}$ are, respectively, the resonance field, swept field, and the full width at half maximum in units of A/m on the abscissa.⁸ On the ordinate we plot the product of the volume static susceptibility χ_0 , the angular frequency ω in Hz and the transverse spin lifetime T_2 in seconds.⁸ The traces

are offset and the base line represents the zero for each trace. Figure 1(a) shows the line shape for χ'' in the absence of magnetic field modulation. The line position would be marked by the field at which the maximum is observed. This relative signal shape has also been shown to be characteristic of the superconducting quantum interference device (SQUID)-detected and Hall-bar detected EPR suppression of the magnetic moment.⁹⁻¹¹ In the presence of field modulation the absorptive signal appears as the first derivative, shown in Fig. 1(b), and the line position is determined by the zero crossing. The first derivative of the reactive signal is illustrated in Fig. 1(c), and the line position is marked as the maximum. Resonant cavity measurements in conjunction with an automatic frequency control that compensates for the

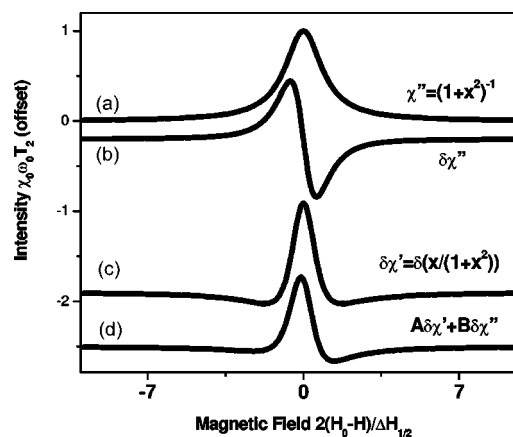


FIG. 1. Simulated spectra based on a Lorentzian line shape and Bloch formalism. (see Ref. 8). The traces are offset with the base line of each representing its zero. (a) Non modulated example of either rf-detected χ'' or dc-detected suppression of χ_0 with arbitrary units. (b) First derivative of (a) representing field modulated χ'' . (c) Field modulated χ' . (d) A mixture of (b) and (c).

^{a)}Author to whom correspondence should be addressed; electronic mail: bcage@boulder.nist.gov

change in resonant cavity frequency can discretely separate these components. However, in the case of transmission measurements using over-moded waveguide, the line is commonly a superposition of these two components. This leads to a mixed spectrum, such as that shown in Fig. 1(d), where it is not clear *a priori* where the line position should be marked or even whether a single peak is present. The methods in use to address this problem are, (a) iterative adjustments of the frequency or phase of the excitation radiation during the experiment until the line shape appears either absorptive or dispersive, (b) post-experimental analytic fitting of the line, or (c), a combination of both.⁷ Unfortunately, these methods entail a certain amount of operator judgment and assumptions as to the signal shape. Another problem with rf-detected transmission techniques is propagation effects, which can be present when the dimension of the sample is close to the wavelength of the exciting radiation.⁷ These effects are described in Ref. 7 as in the case of a plane parallel solid sample where the transmitted power through the faces perpendicular to the propagation direction result in Fabry-Pérot-like interference fringes.⁷ These propagation effects are affected by the (a) sample thickness, (b) magnetic field, (c) radiation frequency and (d) any other perturbations of the refractive index.⁷

Here, we present a SQUID-based multi-frequency EPR method with consistent line shapes that are independent of small experimental changes in phase and frequency. No operator judgment of the spectrum is required and, thus, little doubt as to the shape, position of the resonant field, or number of peaks exists. Additionally, the SQUID detected technique does not directly detect the transmitted rf, and thus, propagation effects are not present.

II. EXPERIMENT

A detailed description of the apparatus is given in Ref. 9; we briefly outline it here. We used a commercial SQUID magnetometer capable of field sweeps from 0 to 7 T and temperature sweeps of 1.8–400 K to obtain the magnetic moment. A klystron operating at 100 mW and 141 GHz was used to generate the microwaves. The power levels used in this experiment are estimated at 25 mW delivered to the sample. We have found that data are obtainable at power levels as low as an estimated 1 mW. There are small line shifts and considerable line broadening at high powers and 1.8 K: these effects are under investigation. The measured sample consisted of a single aligned $[\text{Fe}_8\text{O}_2(\text{OH})_{12}(1,4,7\text{-triazacyclononane})_6]\text{Br}_8 \cdot 9\text{H}_2\text{O}$ crystal, denoted as Fe_8 . The Fe_8 crystal was grown by the typical method¹² and had a volume of approximately 3 mm³. The dc magnetic field was applied along the z axis, z being the high symmetry magnetic axis.

III. RESULTS AND DISCUSSION

Fe_8 is one of the best known single-molecule nanomagnets and has been extensively characterized.^{3,12–18} These studies have determined that the electronic ground state is $S=10$ where S is the primary electronic spin quantum number with an excited state $S=9$ about 24 K above. There are

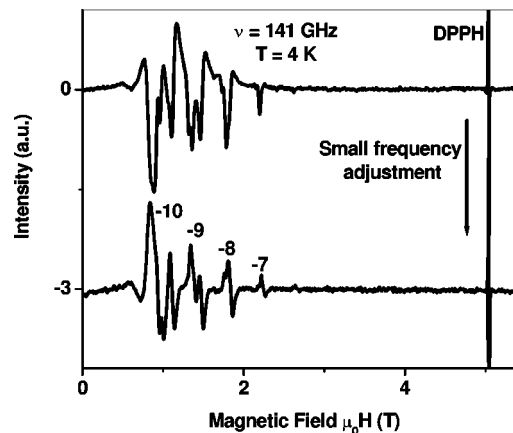


FIG. 2. RF-detected HF-EPR spectra of an Fe_8 single crystal with H parallel to z at 141 GHz and 4 K.

$2S+1 M_s$ energy levels ($-10, -9, \dots, 9, 10$), where M_s is the secondary quantum number for the z component of the electron spin angular momentum. In general, this compound is modeled as a double-well potential with the ten negative M_s levels on one side and the ten positive M_s on the other.

Shown in Fig. 2 are the spectra of a single aligned crystal of Fe_8 obtained with a conventional transmission HF-EPR system at 141 GHz and 4 K. The upper trace shows a spectrum with no operator influence. The lower trace shows the spectrum after iterative operator adjustments of the frequency until the spectrum appears to contain as few dispersive elements as possible. A series of peaks are assigned to the $S=10$ ground state. The peaks are labeled with numbers representing the angular momentum eigenvalues, M_s , from which the spins are excited by the $\Delta M_s=1$ transition, i.e., $M_s=-10$ represents the transition from $M_s=-10$ to -9 . Additional structure in the spectra is sample dependent with unclear origins.¹⁸ A comparison of the upper and lower traces shows that small changes in experimental conditions ($\Delta\nu \approx 100\text{--}500$ MHz) result in very different spectra. This variability in the spectra creates a degree of uncertainty as to where to mark with field positions. The observed peak positions are consistent with the eigenstates and known literature values of the spin Hamiltonian^{13–18}

$$\mathcal{H} = \mu_B g H \cdot S + D S_z^2 + E(S_x^2 - S_y^2) + B_4^0 O_4^0, \quad (1)$$

where μ_B is the Bohr magneton, g is the Lande g tensor, H is the applied magnetic field, D is the uniaxial spin-spin coupling parameter, E is a measure of the magnetic anisotropy in a plane perpendicular to the easy (z) axis of magnetization, S_x , S_y , and S_z are projections along the hard, intermediate and easy axes of the electronic spin operator S , respectively, and the fourth order term is described in Refs. 15–18.

In Fig. 3 we present the magnetization data of Fe_8 in the absence (upper curve) and presence (lower curve) of microwave irradiation at 4 K and 141 GHz. In the absence of microwaves a simple saturation curve is measured. Upon irradiation a series of dips in the magnetization appear. These dips correspond to electron paramagnetic resonant absorption of microwave power between adjacent M_s levels. The inset shows the percent saturation which is equal to $(1 - M_{\text{on}}/M_{\text{off}}) \times 100$ where M_{on} and M_{off} are, respectively, the

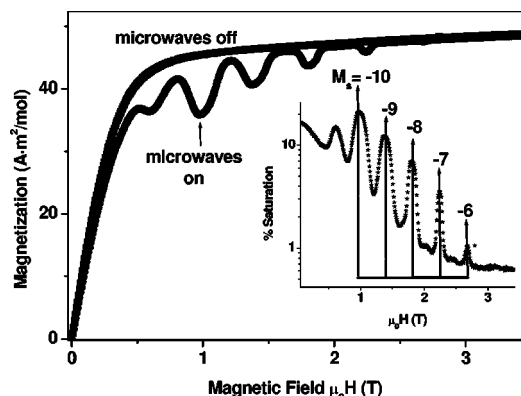


FIG. 3. Magnetization of a single aligned crystal of Fe_8 , with H parallel to z , as a function of magnetic field and microwave irradiation at 4 K and 141 GHz. The upper trace is in the absence of microwaves and the lower trace is in the presence of microwaves. The inset shows a semilog plot of the percent saturation as a function of swept field.

z -axis magnetization (M_z) in the presence and absence of microwave irradiation. In contrast to the transmission data, however, there are clear maxima and little ambiguity exists as to where to mark the peak positions. *These peak amplitudes represent quantitative knowledge of the degree of saturation of the magnetization as function of M_s .* This type of quantitative knowledge is not easily obtained by conventional HF-EPR. The values obtained for this suppression are much larger than those expected for a simple transition between adjacent M_s levels ($<5\%$). We estimate from dc susceptibility data that for the $M_s = -10$ transition in Fig. 3 a temperature increase of ~ 4 K would be needed for the observed 20% reduction in M_z . This is currently under investigation. As the power levels are approximately the same between the rf and dc detected techniques, any potential heating effects on linewidth or line position should affect both equally. The small wiggles at higher fields are consistent with transitions in the $S=9$ excited state.¹⁷ The stick diagram shows the calculated line positions according to Eq. (1) using the standard literature values $g=2.00$, $D=-0.29$ K, $E=0.047$ K and $B_4^0=1.0 \times 10^{-6}$ K.¹⁴⁻¹⁸

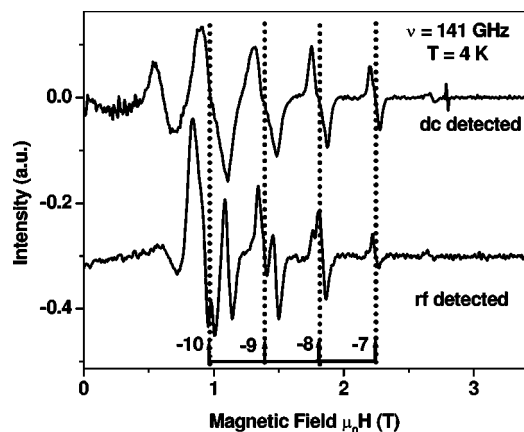


FIG. 4. A direct comparison of the derivative of the dc-SQUID-detected spectrum from the inset of Fig. 3 to the lower trace of Fig. 2

In Fig. 4 we directly compare the rf-transmission-detected and SQUID-detected data. In the upper trace we plot the derivative of the data in the inset to Fig. 3 and in the lower trace we plot the lower trace of Fig. 2. The stick diagram shows the calculated line positions. Little ambiguity exists as to where to mark the line positions of the SQUID detected, whereas a large degree of uncertainty, especially in the transitions at lower fields, exists for the rf-detected lower trace.

IV. CONCLUSION

We have demonstrated that SQUID-based HF-EPR provides a quantitative determination of the dc magnetic moment of nanomagnetic materials as a function of known microwave irradiation power, and removes uncertainties in the line positions and line shapes that arise in standard single-pass transmission HF-EPR. This design should be amenable to perform an rf-detected reflection EPR experiment followed by a SQUID-based EPR experiment thus enabling separation of the dispersive and absorptive elements for questionable spectra.

ACKNOWLEDGMENTS

The authors acknowledge NSF Grant No. DMR/NIRT 0103290 for financial support at FSU, and R. B. Goldfarb of NIST for help with the SQUID magnetometer and valuable discussions.

- ¹B. Cage, A. Hassan, L. Pardi, J. Krzystek, L.-C. Brunel, and N. Dalal, *J. Magn. Reson.* **124**, 495 (1997).
- ²F. Muller, M. A. Hopkins, N. Coron, M. Grynberg, L. C. Brunel, and G. Martinez, *Rev. Sci. Instrum.* **60**, 3681 (1989).
- ³S. Hill, N. S. Dalal, and J. S. Brooks, *Appl. Magn. Reson.* **16**, 237 (1999).
- ⁴W. B. Lynch, K. A. Earle, and J. H. Freed, *Rev. Sci. Instrum.* **59**, 1345 (1988).
- ⁵A. K. Hassan, L. A. Pardi, J. Krzystek, A. Sienkiewicz, P. Goy, M. Rohrer, and L. C. Brunel, *J. Magn. Reson.* **142**, 300-312 (2000).
- ⁶M. Mola, S. Hill, P. Goy, and M. Gross, *Rev. Sci. Instrum.* **71**, 186-200 (2000).
- ⁷L. C. Brunel, A. Caneschi, A. Dei, D. Friselli, D. Gatteschi, A. K. Hassan, L. Lenci, M. Martinelli, C. A. Massa, L. A. Pardi, F. Popescu, I. Ricci, and L. Sorace, *Res. Chem. Intermed.* **28**, 215 (2002).
- ⁸G. E. Pake and E. M. Purcell, *Phys. Rev.* **74**, 1184 (1948).
- ⁹B. Cage and S. Russek, *Rev. Sci. Instrum.* **75**, 4401 (2004).
- ¹⁰W. Wernsdorfer, A. Muller, D. Mailly, and B. Barbara, *cond-mat/0404410* (2004); *Europhys. Lett.* **66**, 861 (2004); E. del Barco, A. D. Kent, E. C. Yang, and D. N. Hendrickson, *Phys. Rev. Lett.* **93**, 157202 (2004).
- ¹¹M. Bal *et al.*, *Phys. Rev. B* **70**, 100408 (2004).
- ¹²K. Wieghardt, K. Pohl, L. Jibril, and G. Huttner, *Angew. Chem., Int. Ed. Engl.* **23**, 77 (1984).
- ¹³C. Delfs, D. Gatteschi, L. Pardi, R. Sessoli, K. Wieghardt, and D. Hanke, *Inorg. Chem.* **32**, 3099 (1993).
- ¹⁴R. Caciuffo, G. Amoretti, A. Murani, R. Sessoli, A. Caneschi, and D. Gatteschi, *Phys. Rev. Lett.* **81**, 4744 (1998).
- ¹⁵A. L. Barra, D. Gatteschi, and R. Sessoli, *Chem.-Eur. J.* **6**, 1608 (2000).
- ¹⁶S. Maccagnano, R. Achey, E. Negusse, A. Lussier, M. M. Mola, S. Hill, and N. S. Dalal, *Polyhedron* **20**, 1441 (2001).
- ¹⁷D. Zipse, J. M. North, N. S. Dalal, S. Hill, and R. S. Edwards, *Phys. Rev. B* **68**, 184408 (2003).
- ¹⁸K. Park, M. A. Novotny, N. S. Dalal, S. Hill, and P. A. Rikvold, *Phys. Rev. B* **65**, 014426 (2002); S. Hill, S. Maccagnano, K. Park, R. M. Achey, J. M. North, and N. S. Dalal, *Phys. Rev. B* **65**, 224410 (2002); S. Hill, R. S. Edwards, S. I. Jones, N. S. Dalal, and J. M. North, *Phys. Rev. Lett.* **90**, 217204 (2003).